

Recent improvements to the Raman-shifted Eye-safe Aerosol Lidar (REAL)

Shane D. Mayor^a, Anna Petrova-Mayor^a,
Bruce Morley^b, and Scott Spuler^b

^aCalifornia State University Chico, Chico, CA 95929

^bNational Center for Atmospheric Research, Boulder, CO 80307

ABSTRACT

Improvements to the original NCAR/NSF Raman-shifted Eye-safe Aerosol Lidar (REAL) made between 2008 and 2013 are described. They are aimed mainly at optimizing and stabilizing the performance of the system for long-term, unattended, network-controlled, remote monitoring of the horizontal vector wind field and boundary layer height, and observing atmospheric boundary layer phenomena such as fine-scale waves and density current fronts. In addition, we have improved the polarization purity of the transmitted laser radiation and studied in the laboratory the effect of the beam-steering unit mirrors on the transmitted polarization as part of a longer-term effort to make absolute polarization measurements of aerosols and clouds.

Keywords: Lidar, wind, aerosol, polarization, boundary layer, clouds, remote sensing, particulate matter

1. INTRODUCTION

In 2005, several of us described the Raman-shifted Eye-safe Aerosol Lidar (REAL) in an SPIE conference paper¹ and subsequently in a 2007 article² in *Optical Engineering*. Since that time, the instrument has been improved in several ways including: (1) installation in a custom field-transportable shipping container; (2) acquisition of new beam steering unit (BSU) mirrors; and (3) implementation of a new transmitter configuration. In addition, we developed an improved data acquisition and control system and added network controllable electronics such as power distribution units and uninterruptable power supplies. While the critical principles of operation of the lidar system remain unchanged (as described in the articles mentioned above and others³), the packaging and maturity of the instrument has improved significantly since 2007. Some of the improvements may not be regarded as novel in and of themselves, but collectively they make the instrument better suited for measurement challenges in the atmospheric sciences. We conclude by suggesting areas for future improvement.

2. FIELD TRANSPORTABLE FACILITY

The instrument was transferred to a new shipping container that was modified to serve as a fieldable experimental lidar facility in 2008. The custom laboratory (left container shown in Fig. 1 and Fig. 2) was designed and fabricated by Design and Fabrication Services (DFS) within the Earth Observing Laboratory (EOL) at the National Center for Atmospheric Research (NCAR). The housing features personnel doors, a roof hatch for the BSU, insulation in the walls, ceiling, and floor, electrical wiring, baseboard heating, and a ductless mini-split type heat pump. The heat pump employs a 10.5 kW compressor/condenser that is mounted in a recessed area on one end of the container. The original double doors of the container may be closed to protect the heat exchanger during shipping. Four air handling units inside are capable of heating and cooling the interior without exchanging air with the outdoors. A custom optics table, 4.26 m long by 1.2 m wide, supports the lidar system (see Fig. 3). The table can be pneumatically isolated to absorb shock and vibration during transit. Moreover, the BSU is now connected to the optics table by a rigid tower made of extruded aluminum and a tip-tilt stage with greater than 40 cm clear aperture. Prior to this configuration, the BSU was fastened to the roof of a much older container and could move with respect to the lidar transmitter and receiver. In the new configuration, a small gap exists between the tip-tilt stage and the roof of the container. The gap is closed with neoprene to

Corresponding author information: sdmayor@csuchico.edu, 530-898-6337.



Figure 1. The Raman-shifted Eye-safe Aerosol Lidar at California State University Chico. (Photo taken May 23, 2013.)

separate outdoor and indoor air and isolate movement of either the roof or the instrument from each other. The new configuration includes the BSU as part of a single rigid instrument.

In addition to the container, several other heavy-equipment components were developed to support the lidar research facility. A 48-foot long trailer was reconditioned to provide a dedicated platform for transport and deployment of the facility. A trailer that is relatively heavy compared to most modern trailers was chosen so that the mass and flat deck (composed of steel and wood planking) provide reduced vibration. Both the new container and the old container that was used for several REAL deployments from 2004 - 2007 are supported by the trailer. The old container is currently used for the storage of tools and parts and as a control room for personnel working at the field site.

A rooftop jib crane was designed by senior undergraduate mechanical engineering students at California State University Chico and fabricated by the College of Engineering Technical Shop. The jib crane is mounted to the roof of the new container and is used to install and remove the BSU. The arm of the crane is 3 m long and the crane is designed to lift up to 227 kg.

3. BSU MIRRORS

In the spring of 2010, the use of a commercially available spray-on/peel-off cleaning product ruined the protected gold coatings of the original BSU mirrors that were described in a 2005 article by Spuler and Mayor.⁴

Those mirrors consisted of 2.54 cm thick octagonal slabs of Zerodur® bonded to 5.08 cm thick honeycomb panels (Teklam A520C). The bond was made using silicon adhesive (GE 167 RTV). The combination resulted in mirrors that were sufficiently flat (< 3 waves peak-to-valley over the clear aperture) and lightweight (15.5 kg). However, the use of glue to bond the Zerodur to the honeycomb panels prevents accurate modeling of the system and it is difficult to remove the Zerodur from the honeycomb panels should they need to be recoated. Here we summarize steps taken since May 2010 to develop an alternative pair of lightweight mirrors. A more detailed description of the effort can be found in Mayor et al. 2011.⁵

Two Gas-Fusion® mirrors were created by Hextek Corp. in 2011-2012. The new mirrors (see Fig. 5) are octagonal shaped with tapered ends and polished to approximately 1 wave flatness across the clear aperture. They are designed to fit within the existing BSU enclosure with the exception of a small portion of the mounting hardware. The three-point mounting system consists of the following parts: (1) a Kovar® puck that is bonded

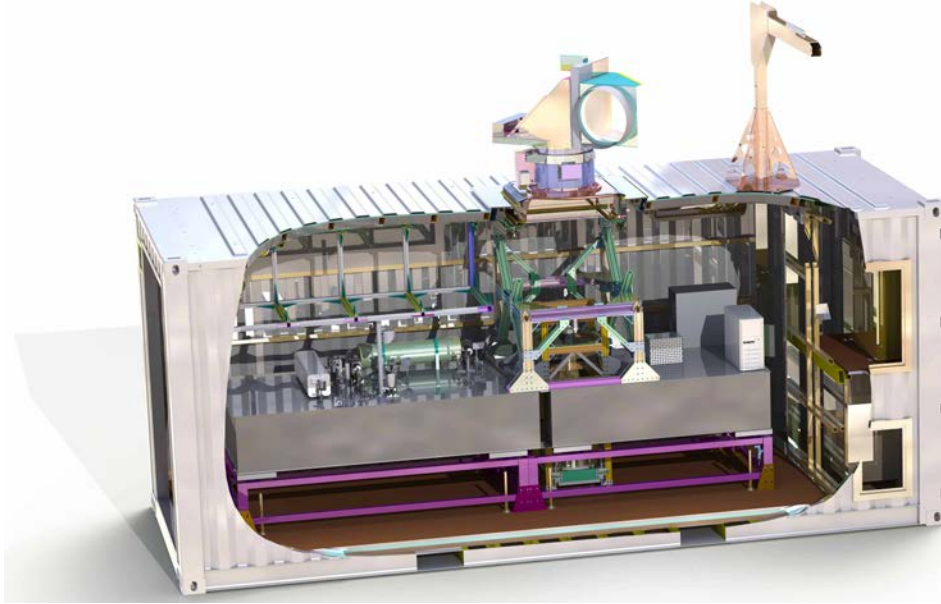


Figure 2. Rendering of a solid model of the REAL that reveals the internal structure.

to the glass using space-grade epoxy. Kovar has a coefficient of thermal expansion which matches that of glass; (2) an I-beam shaped “flexure stage” and (3) a “cup” that connects the flexure stage to the aluminum BSU enclosure panel. The soft-axis of each flexure stage is directed toward the center of the mirror area so that temperature changes between the exterior walls of the BSU and the interior glass cause the flexure stage to bend and minimize stress in the glass. The BSU is wrapped in foil-covered bubble-wrap to minimize heat load through solar radiation. However, the exterior temperatures are easily in excess of 38°C while we strive to keep the inside of the lidar container between 25° and 27°C . Measurements of the BSU substrate temperature have not yet been made to estimate the actual stress that may be imparted in the glass.

The Gas-Fusion mirrors were coated by L&L Optical Services in Los Angeles, CA. The coatings were designed for maximum reflectivity and durability at 1.54 microns wavelength at a 45° angle of incidence. This was accomplished using a layer of gold followed by two overcoats for enhancement. Tests of the mirrors indicate they are approximately 99.0% reflective at 1.54 microns wavelength at a 45° angle of incidence. Reflectivity of the BSU mirror coatings can have a significant impact on the overall system performance. This is because of two sequential reflections for the outgoing pulse in addition to two sequential reflections for the returned radiation. Therefore, if the new mirrors are 99.0% reflective, we expect a 4% (0.99^4) loss due to the BSU while old mirrors that may have been 96.0% reflective, would have resulted in a 15% loss.

4. TRANSMITTER CONFIGURATIONS AND POLARIZATION

Mayor et al. 2007 showed relative backscatter depolarization ratio measurements of aerosol plumes composed of wet and dry particles. However, the measurements were not absolute and only relative changes in depolarization effect of the particles were observed. The reason for that was the inadvertent angle (128° and not 90°) at which the beam generated from the lidar transmitter was projected onto the launch mirror which directs the beam into the BSU (see Fig. 6). This known shortcoming (mainly the result of a space constraint in the old container) resulted in elliptical polarization entering the BSU, whereby it was modified again by the two mirrors of the BSU.

Figure 6 shows the configuration of the lidar’s optics table for the work that resulted in Mayor et al. (2007).² Upon arrival in Chico, CA, in 2008, the components were moved to the new and much larger optics table and the final angle made to project the transmit beam over to the launch mirror was reduced to 77° as shown in Fig. 7. Finally, in January of 2013, the transmitter configuration was arranged so that the beam makes only 90° turns

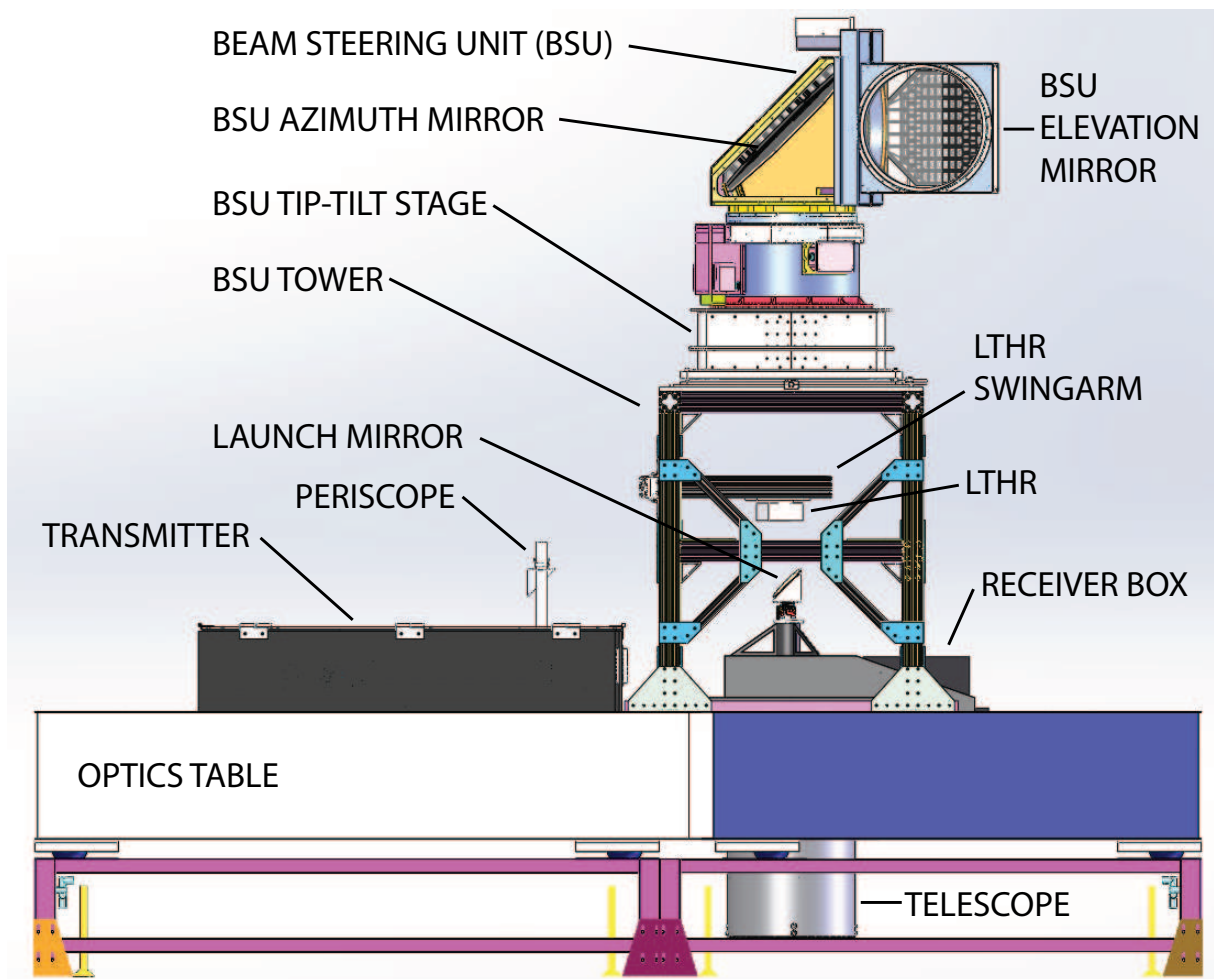


Figure 3. Side view of the instrument. The transmitter and receiver are installed on the top of the optics table and inside enclosures. A square cut-out in the optics table directly beneath the BSU provides an opening to suspend the 40-cm diameter Newtonian telescope with the primary mirror near the floor and the secondary mirror just above the table top. The transmit laser beam is projected from a periscope over to a launch mirror that is mounted in the shadow of the telescope's secondary mirror. A rigid tower connects the optics table to the BSU tip-tilt stage. The BSU is mounted on top of the BSU tip-tilt stage. A lateral-transfer hollow retroreflector (LTHR) is mounted to a retractable swing arm that can be deployed to speed coalignment of the transmitted beam and receiver field of view.

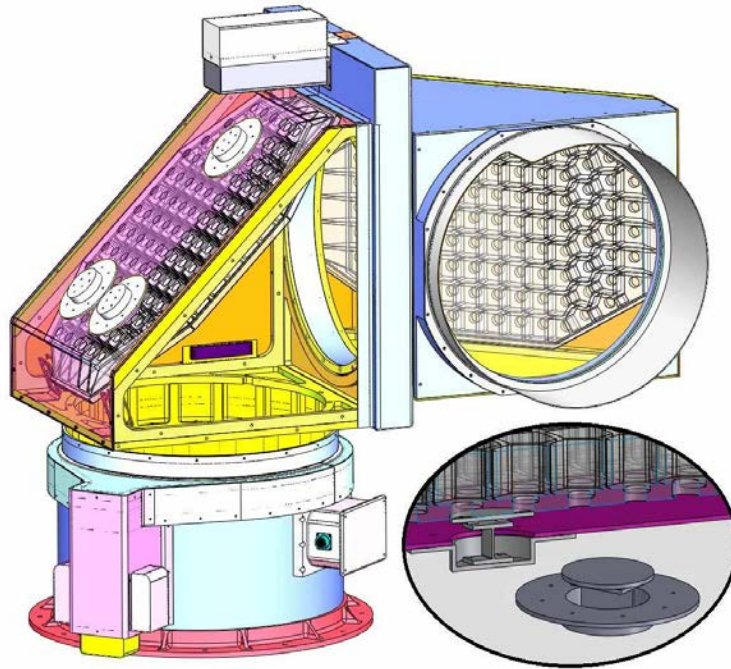


Figure 4. Semi-transparent rendering of the REAL BSU with Gas-Fusion mirrors.

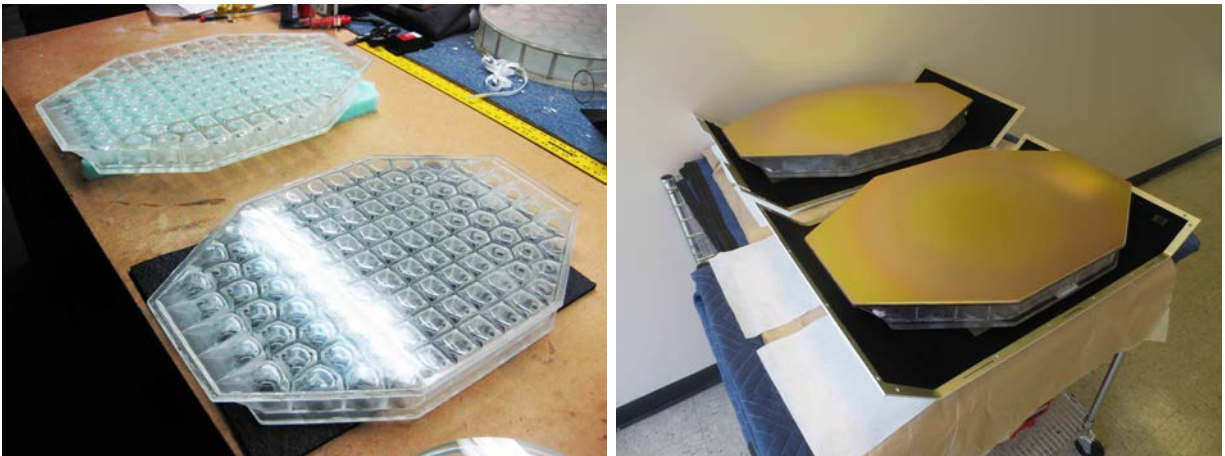


Figure 5. Hextek Gas-Fusion mirrors (left) before polishing and coating and (right) after polishing and coating.

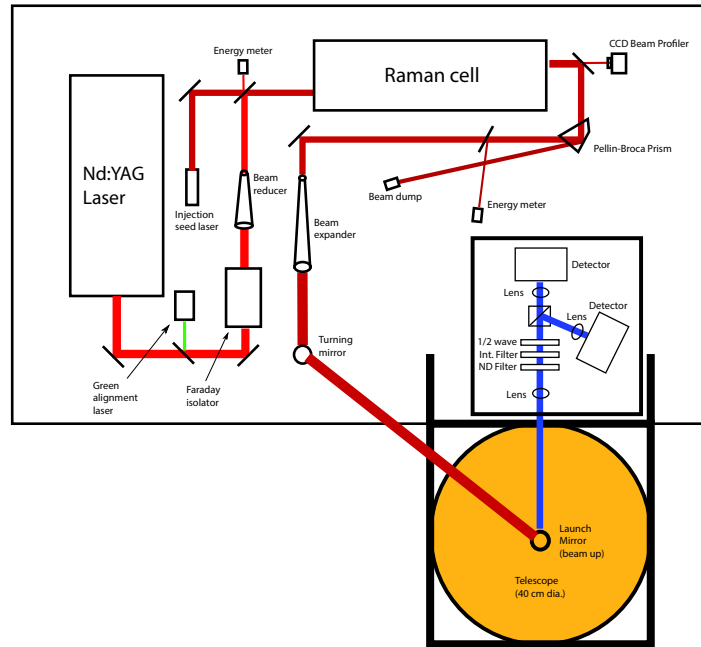


Figure 6. Top-down view of the arrangement of optical components (prior to 2008) that resulted in elliptical polarization of the transmitted pulses prior to the BSU. Depolarization ratio results presented in Mayor et al. (2007)² were collected with the instrument in this configuration.

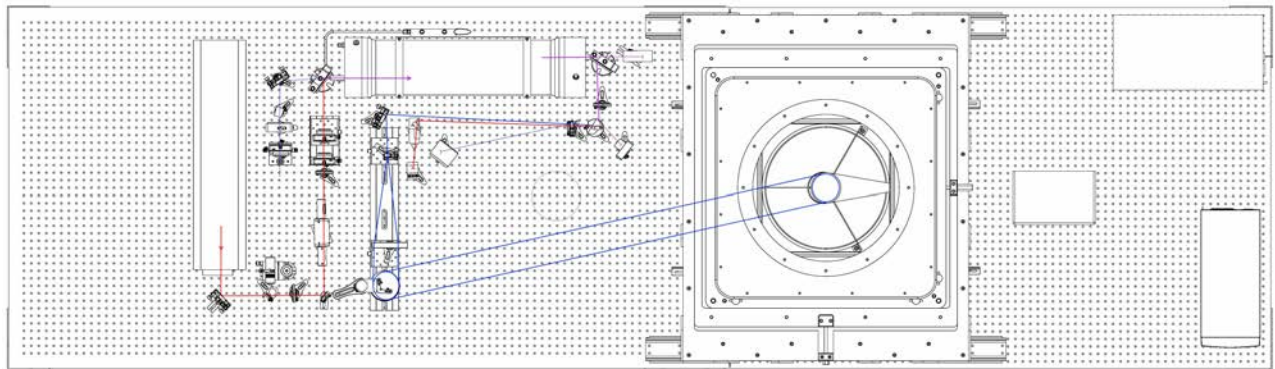


Figure 7. Top-down view of the arrangement of optical components (between 2008 and January 2013) that resulted in elliptical polarization of the transmitted pulses prior to the BSU.

before reaching the launch mirror as shown in Fig. 8. Furthermore, we replaced all kinematic mirror mounts with Newport VGM-1 and VGM-2 gimbal mounts. Several additional beam blocks (Thorlabs LB-1) were used to stop higher order reflections from mirrors and the Pellin-Broca prism in the system. We find that using gimbal mounts creates a sturdier system that is more easily aligned, and the careful placement of the additional beam blocks appears to reduce unwanted noise in the pulse energy measurement.

5. ALIGNMENT OF TRANSMIT BEAM AND RECEIVER FOV

The REAL is a monostatic coaxial lidar system. The transmit beam is projected into the receiver's field of view (FOV) by a 10 cm diameter turning mirror that is mounted in the shadow of the receiver telescope's secondary mirror. In the past, alignment of the transmit beam into the receiver's FOV was a challenge. This is because

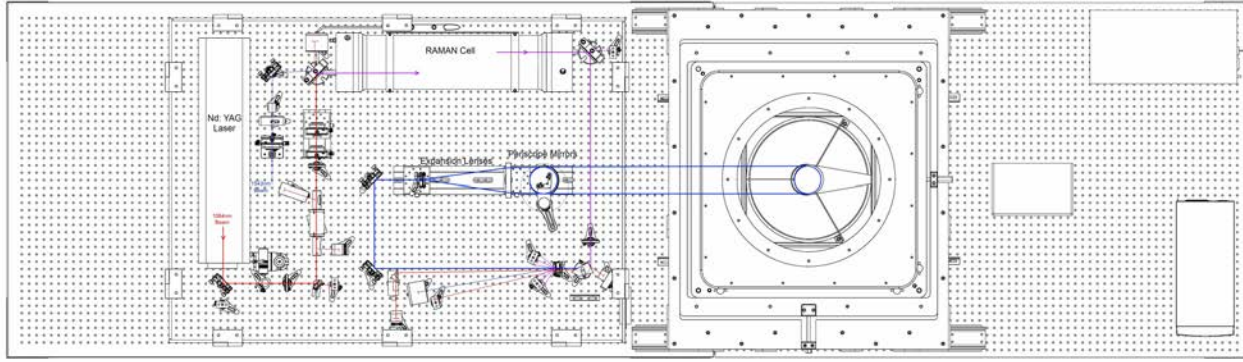


Figure 8. Top-down view of the arrangement of optical components (after January 2013) that maintain linear polarization of the transmitted pulses prior to the BSU.

the transmit beam and receiver FOV are defined entirely by independent sets of optical mounts. A successful alignment could be achieved by either “walking” the transmit beam into the receiver’s FOV and/or moving the photodetectors. Both of these processes involve moving components with micrometers to maximize the detected backscatter signal. The difficulty lies in the inability to “see” the FOV subtended by the detectors and move the transmit beam into it. It is a slow procedure that requires patience and continuous subjective judgments as to whether the signal is improving or weakening.

To speed the alignment process, we purchased and installed a lateral transfer hollow retroreflector (LTHR) from PLX Inc. The LTHR is mounted on an extruded aluminum swing arm that can easily be moved into place to bring the transmitter and receiver subsystems into alignment. When set in place for an alignment, the LTHR returns a portion of the transmit beam directly into the receiver’s telescope primary with less than 30 arcseconds (0.0083°) of parallelism to the transmit beam above the launch mirror. The LTHR has 2.54 cm clear apertures and the displacement between the input and output beams is 10.16 cm. When in position, system engineers can easily steer the beam returned by the LTHR to the entrance of the receiver subsystem by adjusting the tip and tilt of the launch mirror and/or telescope primary mirror.

6. POLARIZATION EFFECTS OF THE BSU

In this section, we describe our efforts to characterize the effects of the BSU on the polarization state of the transmitted laser radiation. We built a miniature BSU (mini-BSU) for use in the lab and used a polarimeter to map the state of polarization (SOP) of the transmit beam for all pointing directions (Fig. 9). The mirrors are witness samples of the large scanner mirrors and are characterized at the same laser wavelength as transmitted by REAL. The REAL has two sets of BSU mirrors—enhanced gold and enhanced aluminum coated. Here, we present the results for the aluminum coated mirrors (currently installed in REAL) when vertical polarization is incident on the launch mirror. We expect similar results for the gold coated mirrors. Figure 10 shows that the linear polarization is preserved only for horizontal scans. However, the polarization ellipse rotates as a function of the azimuth angle. Also, the SOP repeats every 180° in azimuth and in elevation. When comparing horizontal to vertical incident polarization on the launch mirror, we found that the corresponding ellipses have the same ellipticity but their orientations are orthogonal to each other.

The effects induced by the BSU mirrors can be partially compensated for by means of altering the incident polarization.³ By rotating a quarter-wave plate (QWP) in front of the launch mirror (hence sending elliptical polarization to the BSU) we achieved linear polarization (canceled the ellipticity) for all scan directions. The orientation, however, remains unchanged. Given that the backscattered signal will suffer the same effects from the mirrors, a QWP must be installed in the receiver as well. Both quarter-wave plates would have to be electronically controlled, synchronized with each other, and linked to the rotation of the BSU mirrors. If a combination of a half-wave plate and a quarter-wave plate is used instead, the transmit polarization can be set to circular for all scan direction. A potentially more elegant and cost effective method would entail removing the effects of the

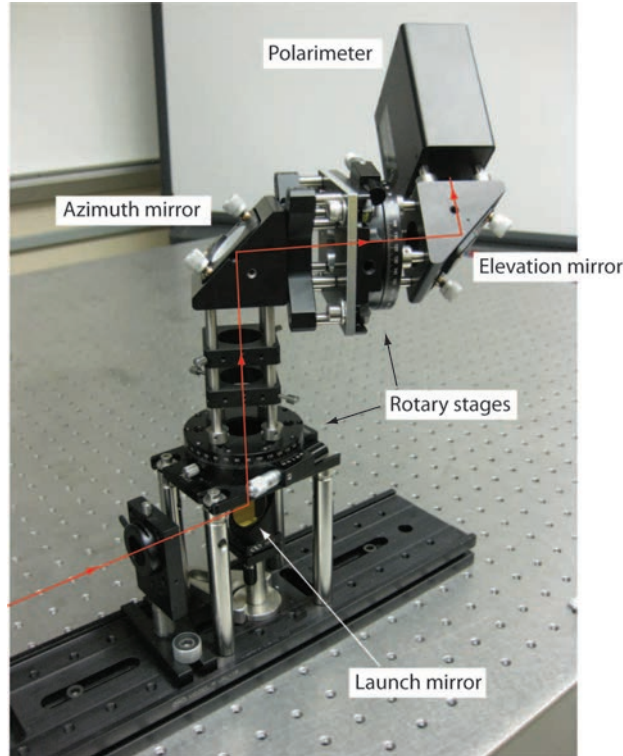


Figure 9. Mini-BSU with polarimeter.

scanning mirrors in post processing. This requires polarimetric characterizations of the mirrors diattenuation and retardance as a function of tilt angle. These quantities are initially obtained from the miniature BSU and can be refined using atmospheric returns. Since the mirror tip and tilt angles are known, the effect of the two mirrors can be consolidated into a 2×2 measurement matrix. This matrix relates the two atmospheric variables (volume backscatter and depolarization) to the two polarization measurement channels.⁶ The measured powers on the polarization channels are then multiplied by the inverse of the measurement matrix to obtain the volume backscatter and depolarization, independent of the BSU mirror effects.

7. REMOTE CONTROL

A requirement for many atmospheric investigations is the ability to operate the lidar continuously and for long periods of time. This necessitates remotely-controllable and unattended operation. For example, one may wish to collect data for use in a wind resource assessment or monitor boundary layer height over one or more seasons. In some applications, such as surveillance, continuous operation is also a requirement.

Continuous operation of the REAL seems to depend mostly on satisfying three conditions: (1) stable interior air temperature; (2) dust-free interior; and (3) no disruption in electrical power. Toward this, we use an IQ Air Health Pro Plus HEPA filter with an Outflow W125 attachment to create a particle-free positive pressure area around the laser transmitter. To prevent brief power disruptions from affecting lidar operation, we installed five APC rackmount uninterruptible power supplies (UPSs). For temperature stabilization, we set the container air conditioning to 22°C and the baseboard heaters to a “low” setting. Six small fans are used to vigorously mix the air inside the container. This summer we have been successful at holding the interior air temperature between 24.6° and 26.5°C while the outdoor air temperature ranges from approximately 15° to 44° . Fluctuations in the interior temperature are strongly correlated with the outdoor temperature and do have an effect on the laser transmitter performance. Currently, we notice an increase in transmit power of about 15 mJ during the night presumably due to cooler interior air temperatures affecting the divergence of the Nd:YAG pump beam and the

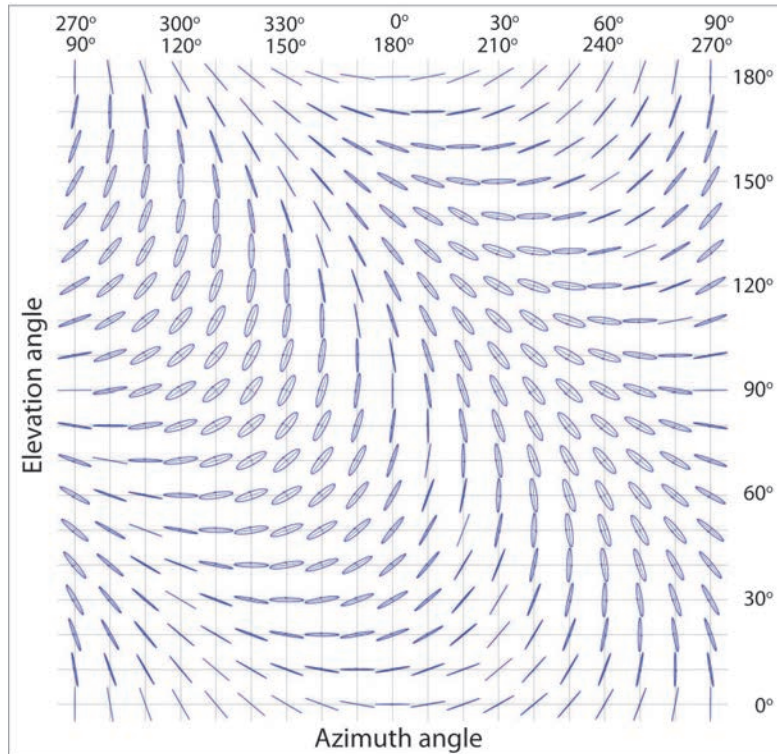


Figure 10. Polarization of the transmitted beam if vertical polarization is incident on the launch mirror.

stimulated Raman scattering conversion efficiency. The REAL transmits between 130 and 170 mJ per pulse. The amount depends on the age of the flashlamps and the flashlamp voltage. The flashlamp voltage has only 11 possible settings that span the range of 1.47 - 1.57 kV in 0.01 kV increments.

In addition to maintaining a stable interior environment, we found that it is necessary to monitor and control many lidar system devices remotely through the network. To do that, we installed network-controllable power distribution units (PDUs) and network management cards in the UPSs. These allow us to cycle the power to various devices if necessary and monitor the status of the UPS and electric utility service. The network management cards instruct the computers to shut down gracefully in the event of a power outage that is long enough to significantly drain the batteries. We've also installed an electronically controlled shutter for the receiver box and a "key-turner" for the Nd:YAG power and cooling unit. These allow us to protect the receiver from inadvertent hard-target reflections and turn the system off and on remotely.

8. COMPUTATIONAL ASPECTS

The REAL currently requires two computers for operation: one for system control and data acquisition and a second for data archive and the production of near-real-time products. The system control computer is a Dell Precision T7500 workstation running Windows 7. It has a single Intel Xeon quad-core E5620 processor at 2.4 GHz and 12 GB of RAM. The lidar system is controlled and data is acquired through a custom LabVIEW® program. Data files are written to two external hard drives in a dock. Original raw data (to 5.8 km range) is saved at a rate of about 25 GB per day.

The second computer in the REAL is a Supermicro server with one 6-core Intel Xeon 5680 at 3.33 GHz processor, 12 GB of RAM, and 32 TB of data storage through the use of eight 4 TB hard drives in a RAID 6 configuration. This rackmount machine currently supports two Nvidia graphical processing units (GPUs): one Tesla C2070 and one Kepler K20. Original data files are copied from the other computer to this machine where the data are used to calculate products such as images and 2-component vector flow fields.

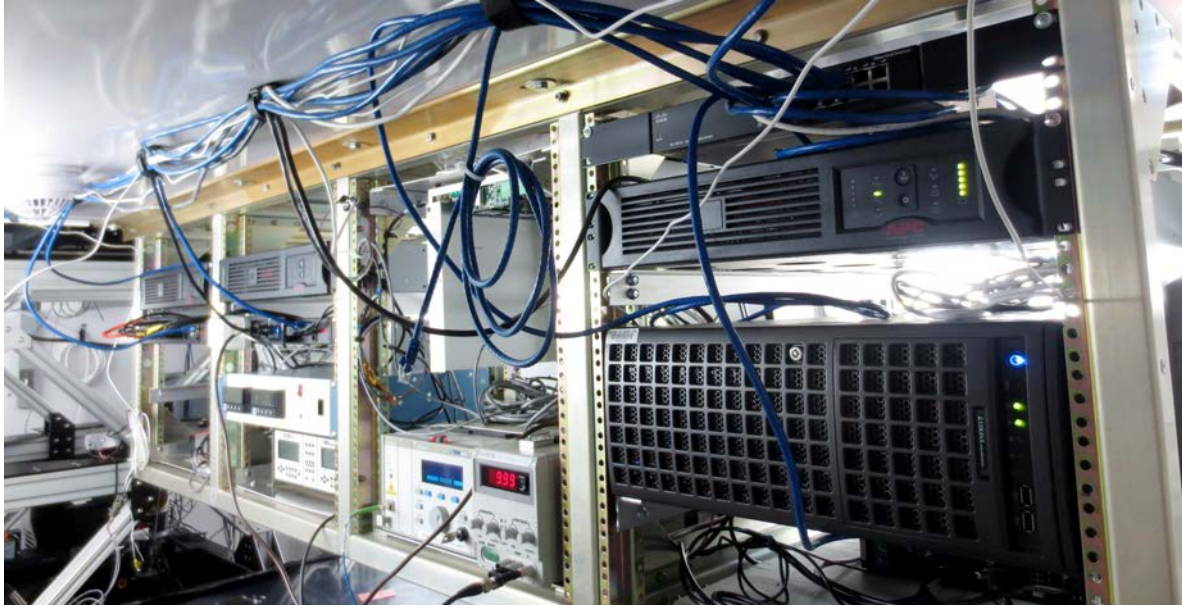


Figure 11. Network controlled uninterruptable power supplies, power distribution units, and a GPU server were added to the REAL.

Several other desktop computer systems running Windows 7 are installed in the REAL as workstations. We use RealVNC® software to enable remote desktop control of the system control and data acquisition computer. All computers and network equipment are connected via gigabit switches and shielded Cat6A cabling. The system is connected to the university computer network via a series of wireless links spanning about 7 km. The bandwidth of the network connection is sufficient that we can easily run the remote desktop software from campus and distant locations (such as Boulder, Colorado).

For much of the research that the REAL is used for, the data must be accurately time-stamped (i.e., comparison of measurements with those from other sensors). Therefore, we installed a GPS network time server (model TM1000A from CSS Time Machines in Lincoln, Nebraska). All clocks on computers and network devices in the lidar system synchronize their clocks with this source. We have found that by synchronizing the data acquisition computer's clock to the GPS time server every 2 minutes, the drift remains less than a few milliseconds. We use Network Time System Softros Systems, Inc. to perform the synchronization on all computers running Windows. The presence of a GPS time server onboard the lidar facility insures that all data are accurately time-stamped regardless of the status of the connection to the internet.

Based on our experience in the 2007 Canopy Horizontal Array Turbulence Study (CHATS)⁷ that was conducted in Dixon, California, we came to realize the importance of maintaining a stable platform. Very small rolls and pitches of the trailer (caused by wind load, personnel walking, or simply expansion and contraction of the trailer from the diurnal cycle of temperature) can displace the laser beam by significant amounts of altitude at distances of interest when scanning horizontally. For our current research experiment that involves comparing REAL measurements with those from other sensors, it is very desirable to have consistent beam positioning, or at least knowledge of any changes. Therefore, we installed two Applied Geomechanics Model 801 Tuff Tilt Uniaxial Tiltmeters that are used to monitor the pitch and roll of the instrument. The tiltmeters sit on the optics table. Each tiltmeter has an angular range of ± 0.5 degrees and a resolution of less than 10^{-4} degrees and a repeatability of less than 2×10^{-4} degrees. The sensors have a time constant of about 1.75 s, and the REAL data acquisition system samples and records their output at the 10 Hz pulse rate of the lidar. In the future, we plan to use these data in real-time to compensate for tip and tilt of the platform for improved stabilization of the lidar beam. Currently, from where the trailer has been parked on firm dry ground for over 5 years, data from the tiltmeters indicate that the trailer rolls and pitches by less than 0.02° over the course of a typical day.

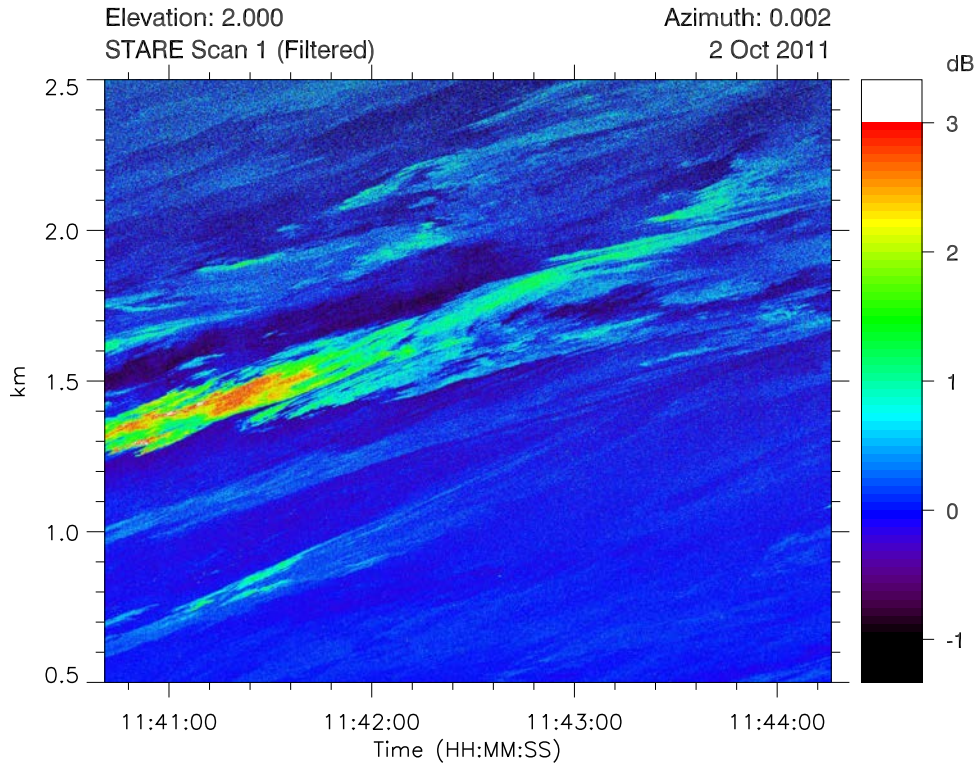


Figure 12. High-pass median-filtered elastic backscatter intensity from a nearly-horizontal stare of the REAL on 2 October 2011. In this 3.75-minute example, the BSU is held stationary and aerosol features are carried through the beam by the wind. The backscatter intensity values at one point in range were compared in situ particle concentration measurements.¹¹

Two-component two-dimensional wind fields are calculated in real-time by applying motion estimation algorithm to sequential pairs of horizontal scans on the GPUs. Descriptions of this work can be found in Mauzey et al. (2012),⁸ Mayor et al. (2012),⁹ and in another paper by Mayor et al. (2013)¹⁰ in this conference.

Finally, an additional significant capability that we have developed is the ability to disseminate digital products such as time-series data, brief animations of recent images of scan data, and vector flow fields in near real-time to the public via the internet. Currently, data products are uploaded to the CSU Chico Department of Physics server and made available through the Atmospheric Lidar Research Group website: phys.csuchico.edu/lidar.

9. FIELD RESULTS

We operate the REAL at the CSU Chico farm routinely for atmospheric investigations. In the autumn of 2011, we, and collaborators from the University of Bayreuth, conducted a small pilot experiment at the CSU Chico farm to explore the feasibility of characterizing the REAL's sensitivity to small changes in the microphysical properties of aerosol particles using in situ sensors. During the experiment, the REAL laser beam was directed horizontally and held stationary across the fields of the farm and aimed to pass within a meter of the inlets of two optical particle counters located at a range of 1.3 km. The results, summarized in a conference paper,¹¹ indicate that such a characterization is indeed feasible. Figure 12 is an example of just a short period of "stare" data collected during the experiment to show the detailed variations in aerosol backscatter that can be detected by the REAL.

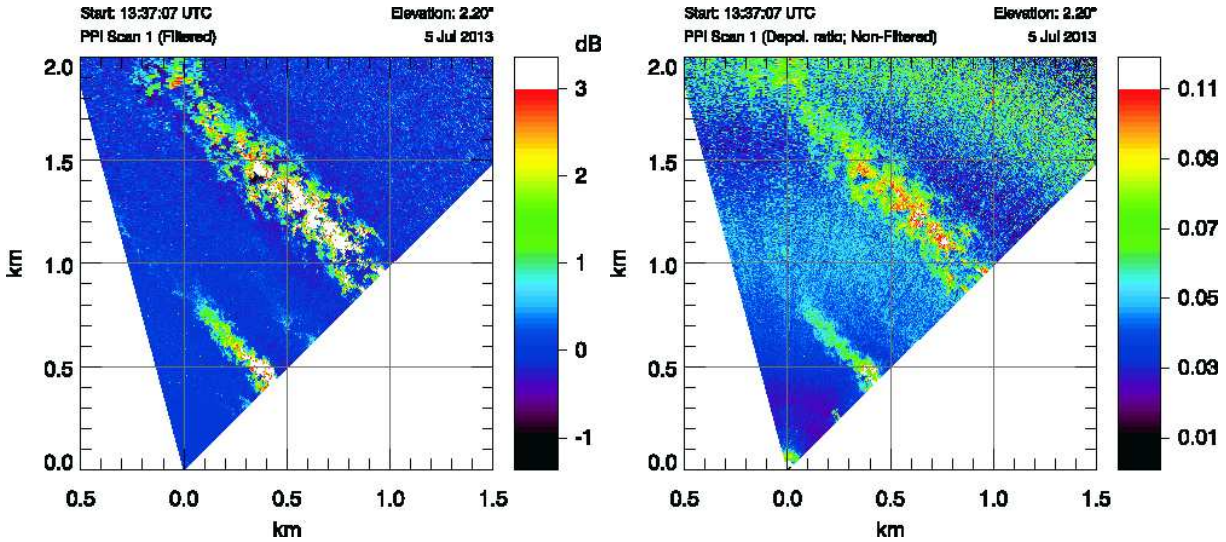


Figure 13. One 60° wide horizontal scan at an elevation angle of 2.20° from the REAL. Left: Range-corrected backscatter intensity after high-pass median filtering. Right: Backscatter depolarization ratio.

The REAL is capable of operating continuously for as long as it takes to discharge approximately 20 million pulses. This is due to the finite lifetimes of Nd:YAG laser flashlamps. Therefore, pulsing at a rate of 10 Hz allows for up to 23 days of continuous lidar operation. Changing flashlamps requires about 30 minutes. As the flashlamps age, the pulse energy decreases and the beam divergence increases. However, this can be compensated for by increasing the flashlamp voltage. Therefore, every few days, we log into the system control and data acquisition computer and increase the flashlamp voltage slightly through the LabVIEW program that controls the lidar system. In 2007, we collected approximately 3 months of nearly continuous data in this fashion at the CHATS experiment. Doing so resulted in spectacular observations of two small-scale phenomena: density current fronts¹² and fine-scale gravity waves.¹³ In late May of 2013, we began collecting nearly-continuous observations in Chico, CA, and continue at the time of this writing (late July). We plan to continue operating continuously through the late autumn of 2013.

Figures 13 and 14 show an example of data collected on 5 July 2013 in Chico, CA. The left panel in Fig. 13 is high-pass median filtered elastic backscatter intensity. The right panel in Fig. 13 shows the backscatter depolarization ratio, computed by dividing the perpendicular channel by the parallel channel signal after subtracting the background levels. Although we do not know the microphysical nature (i.e., the size distribution or shapes) of the particles making up the background and plumes in these images, we note that the range of depolarization ratios (0.10 to 0.11) is much lower than in our previous study² and closer to values published elsewhere.

Figure 15 shows an example of another measurement capability of the REAL. The top panel in the figure shows one vertical scan, collected in about 9 s from approximately 0° to 35° elevation. The convective boundary layer (CBL) height has been estimated as a function of horizontal distance from the lidar by applying a Haar wavelet transform as described by Davis et al.¹⁴ The lidar data, in its native spherical coordinate system with azimuth held constant, is interpolated on to a Cartesian grid with axes in horizontal distance and altitude. The algorithm is applied to each column of the Cartesian grid data where it identifies a large-scale step-like change in the backscatter signal intensity. After being applied to each column, the locations of the CBL heights are binned as a function of altitude, and the bin containing the largest number of counts (the median) is chosen as a measure of the CBL depth for that scan. A time-series of CBL heights (lower panel in Fig. 15) can be created by collecting RHI scans continuously or periodically and applying the above procedure. In this case, we see that the CBL grew from 500 m AGL at 14 UTC (6 AM PST) to more than 1 km AGL at 18 UTC (10 AM PST) and varied through the rest of the day.

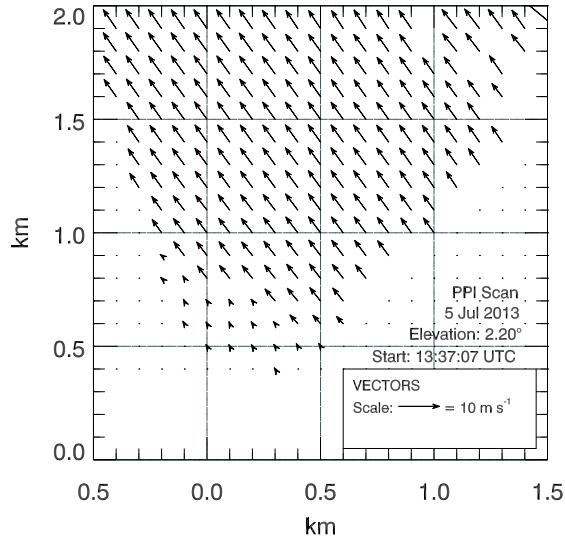


Figure 14. Aerosol motion vectors that estimate the two-component wind field. This vector flow field was calculated from the left image shown in Fig.13 and the subsequent scan that occurred 17 s later.

10. FUTURE WORK

Several improvements could be made to the REAL to dramatically improve its performance and make it easier to use especially for applications requiring long-term unattended measurements. Some of these are described in Mayor (2010).¹⁵ First, replacement of the transmitter with an all-solid-state laser and wavelength converter is highly desirable for continuous long-term operation. However, it is important to note that REAL currently achieves its performance by transmitting sufficient energy in each individual pulse to generate good signal-to-noise backscatter to ranges of several kilometers without any multi-pulse averaging. We believe this could be achieved with the use of diode pumping (instead of flashlamps) and the use of non-linear optical materials (instead of the Raman cell) in a fashion similar to what was demonstrated by Webb et al.¹⁶ We note that higher pulse energy and higher pulse repetition rate are possible while maintaining eye-safety by expanding the diameter of the transmit beam. Doing so maintains acceptable energy density in the transmit beam. Similarly, the diameter of the telescope could be increased. A higher pulse repetition rate (without decreasing pulse energy) would enable faster scanning and translate to improved aerosol motion estimates. Increased pulse energy and larger receiving optics would improve the backscatter signal-to-noise ratio and result in improved performance at longer ranges.

The Gas-Fusion BSU mirrors described in section 3 have not been installed in the REAL at the time of this writing. We hope to do that by the end of the calendar year. Other improvements that we plan to implement in the near future include: (1) Upgrading the system control and data acquisition computer and software with hardware and software that operates under the LabVIEW real-time operating system (RTOS). The current system is limited to data acquisition at 10 Hz pulse rate; (2) Testing and possible replacement of the Perkin Elmer C30659-1550-R2A avalanche photodiodes (APDs) with newly available APDs that offer lower noise; and (3) Using the platform roll and pitch information to adjust the BSU pointing direction to maintain precise beam altitude at distance ranges. In the future, we wish to deploy the REAL at a coastal location in order to scan over the ocean and retrieve horizontal and vertical spatial profiles of wind speed, direction, and atmospheric boundary layer height.

ACKNOWLEDGMENTS

The REAL was developed at the National Center for Atmospheric Research (NCAR) that is supported by the National Science Foundation (NSF). Since moving to CSU Chico in 2008, the work has been supported by NSF Awards 0924407, 1104342, and 1228464. Many individuals from NCAR and CSU Chico and beyond have provided critical assistance. Special thanks to the CSU Chico College of Agriculture, CSU Chico College of Engineering, Mr. Denton Scott, Dr. Eric Ayars, Mr. Patrick Ponsardin, and Dr. Matthew Hayman.

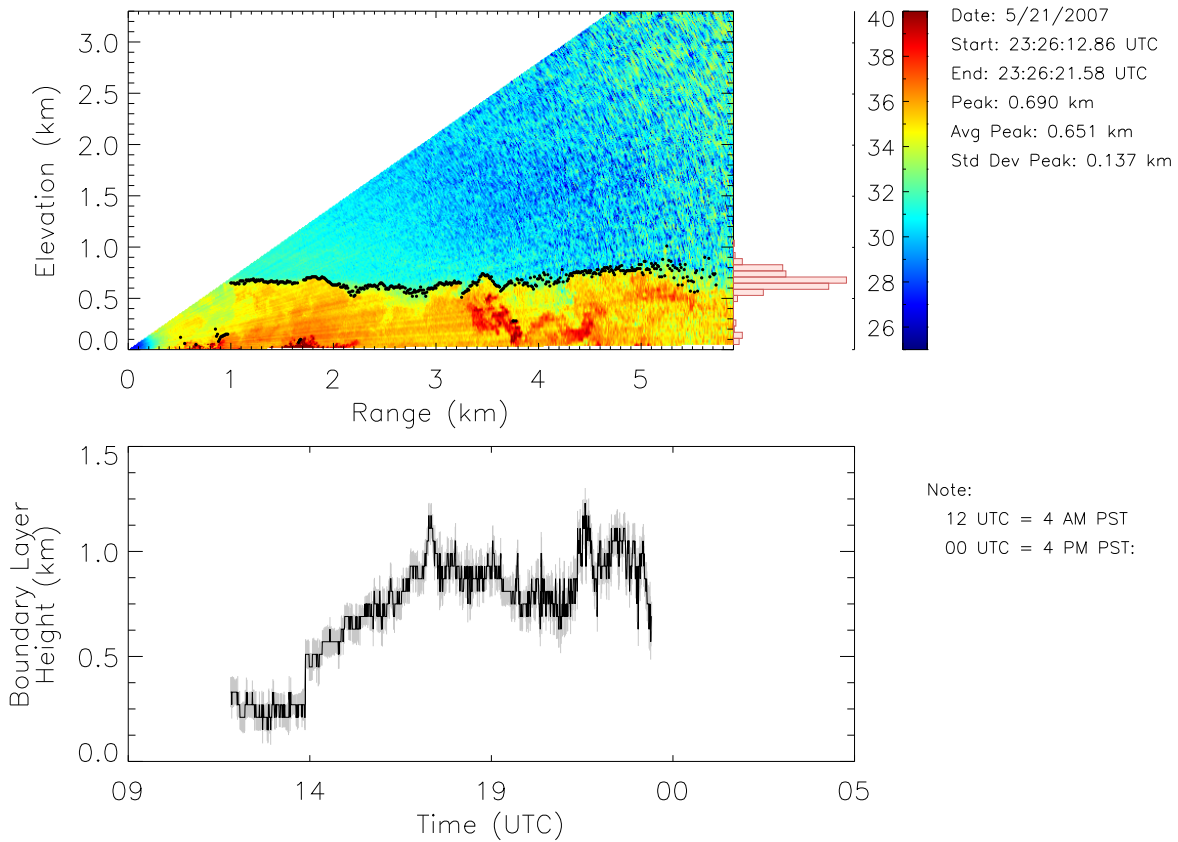


Figure 15. Top panel: One vertical scan from the REAL on 21 May 2007 at 23:26 UTC revealing the atmospheric convective boundary layer (CBL). An algorithm was applied to objectively identify the altitude of the top edge of the CBL in the image. The location of the top edge is delineated by the black dots superimposed on the image and a histogram of the number distribution is shown on the right side. The maximum of the distribution is a way of providing a single measure of the boundary layer height for the entire scan. Bottom panel: The above procedure can be applied for all vertical scans during the course of a day resulting in a time-series of boundary layer heights. Here we see growth of the CBL during the morning hours and substantial variation in the CBL height during the afternoon.

REFERENCES

- [1] Mayor, S. D., Spuler, S. M., and Morley, B. M., “Scanning eye-safe depolarization lidar at 1.54 microns and potential usefulness in bioaerosol plume detection,” in [*Lidar Remote Sensing for Environmental Monitoring VI*], Paper 5887–23, SPIE (2005).
- [2] Mayor, S. D., Spuler, S. M., Morley, B. M., and Loew, E., “Polarization lidar at 1.54-microns and observations of plumes from aerosol generators,” *Opt. Eng.* **46**, DOI: 10.1117/12.781902 (2007).
- [3] Gimbal, S., Li, Q., and Petrova-Mayor, A., “Polarization effects induced by a two-mirror laser beam scanner,” in [*Proc. SPIE, Remote Sensing System Engineering IV*], **8516**, 85160F–85160F–8 (2012).
- [4] Spuler, S. M. and Mayor, S. D., “Scanning eye-safe elastic backscatter lidar at 1.54 microns,” *J. Atmos. Ocean. Technol.* **22**, 696–703 (2005).
- [5] Mayor, S. D., Petrova-Mayor, A., Wortley, R. W., Hofstadter, D. S., Spuler, S. M., and Ranson, J., “Gas-fusion mirrors for atmospheric lidar,” in [*Frontiers in Optics(FiO)/Laser Science(LS)*], Optical Society of America (2011). Poster Presentation JTUA19, 16-19 Oct. 2011, San Jose, CA.
- [6] Hayman, M., Spuler, S., Morely, B., and VanAndel, J., “Polarization lidar operation for measuring backscatter phase matrices of oriented scatterers,” *Opt. Express* **20**, 29554–29567 (2012).
- [7] Patton, E. G., Horst, T. W., Sullivan, P. P., Lenschow, D. H., Oncley, S. P., Brown, W. O. J., Burns, S. P., Guenther, A. B., Held, A., Karl, T., Mayor, S. D., Rizzo, L. V., Spuler, S. M., Sun, J., Turnipseed, A. A., Allwine, E. J., Edburg, S. L., Lamb, B. K., Avissar, R., Calhoun, R., Kleissl, J., Massman, W. J., U, K. T. P., and Weil, J. C., “The Canopy Horizontal Array Turbulence Study (CHATS),” *Bull. Amer. Meteor. Soc.* **92**, 593–611 (2011).
- [8] Mauzey, C. F., Lowe, J. P., and Mayor, S. D., “Real-time wind velocity estimation from aerosol lidar data using graphics hardware,” GPU Technology Conference, San Jose, CA (May 2012). Poster presentation AV10.
- [9] Mayor, S. D., Lowe, J. P., and Mauzey, C. F., “Two-component horizontal aerosol motion vectors in the atmospheric surface layer from a cross-correlation algorithm applied to elastic backscatter lidar data,” *J. Atmos. Ocean. Technol.* **29**, 1585–1602 (2012).
- [10] Mayor, S. D., Dérian, P., Mauzey, C. F., and Hamada, M., “Two-component wind fields from scanning aerosol lidar and motion estimation algorithms,” SPIE (August 2013). Paper 9972-7.
- [11] Held, A., Seith, T., Brooks, I. M., Norris, S. J., and Mayor, S. D., “Intercomparison of lidar aerosol backscatter and in-situ size distribution measurements,” (September 2012). Presentation number B-WG01S2P05, European Aerosol Conference, Granada, Spain.
- [12] Mayor, S. D., “Observations of seven density current fronts in Dixon, California,” *Mon. Wea. Rev.* **139**, 1338–1351 (2011).
- [13] Randall, T. N., Jachens, E. R., and Mayor, S. D., “Lidar observations of fine-scale atmospheric gravity waves in the nocturnal boundary layer above an orchard canopy,” AMS (July 2012). P33 in 20th Symp. Boundary Layers and Turbulence, Boston.
- [14] Davis, K. J., Gamage, N., Hagelberg, C. R., Kiemle, C., Lenschow, D. H., and Sullivan, P. P., “An objective method for deriving atmospheric structure from airborne lidar observations,” *J. Atmos. Ocean. Technol.* **17**, 1455–1468 (2000).
- [15] Mayor, S. D., “High pulse-energy atmospheric aerosol lidar at 1.5-microns wavelength: Opportunities for innovation from a meteorologists perspective,” OSA (May 2010). Conference on Lasers and Electro-Optics (CLEO) and the Quantum Electronics and Laser Science Conference (QELS), JThJ2, San Jose, CA.
- [16] Webb, M. S., Moulton, P. F., Kasinski, J. J., Burnham, R. I., Loiacono, G., and Stolzenberger, R., “High-average-power KTiOAsO₄ optical parametric oscillator,” *Opt. Lett.* **23**, 1161–1163 (1998).